This is a repository copy of *Benchmarking of premium rail material wear*.

BENCHMARKING OF PREMIUM RAIL MATERIAL WEAR

P. Christoforou[*], S.R. Lewis, D.I. Fletcher, R. Lewis

Department of Mechanical Engineering, University of Sheffield, UK

* pchristoforou1@sheffield.ac.uk

ABSTRACT

Railway steel that offers a greater quality and extended life is described by the industry as premium rail. It is mainly used on areas of rail networks where accelerated wear, RCF or other rail related damage phenomena prevail. However, little performance data exists for these materials and where it does it is limited to one set of contact conditions. The aim of this work was therefore to map premium rail performance across a range of $T\gamma$ contact conditions to benchmark against standard grade R260 rail. Laboratory tests using a twin disc machine were performed to determine the wear performance of four premium rail grades against R8 wheel material, at various slip conditions of 1-20%. The results are shown in terms of $T\gamma$ and cyclic wear rate for both the rail and wheel discs. Material hardness mapping was obtained as a comparison between the full rail and the laboratory small scale specimen materials in order to correlate hardness with their wear behaviour. The purpose of this work is to understand the likelihood of wear in different wheel/rail contact conditions and to produce enough wear information for the premium rail that could be used in prediction tools for comparison with other materials and contact conditions.

Keywords: wear; RCF; rolling-sliding; laser cladding; twin disc; hardness; premium rail;

1. INTRODUCTION

The demand for faster and safer railways promotes the development of railway steel with greater quality and extended life. Such steel is described by the industry as premium rail and is mainly used on areas of rail networks where accelerated wear, RCF (rolling contact fatigue) or other rail related damage phenomena prevail. It is important to evaluate new materials used for rail since its performance may affect the other component of the interface, the wheel. Different types of wheel material and dimensions/profiles are being used on railways with a combination of varying loads and conditions. Wear mapping of materials is common practice in research [1, 2] and enables tribologists to identify material wear behaviour for example by mapping wear rate against $T\gamma/A$ or using an Archard wear coefficient approach [3]. This provides a standalone tool for understanding the likelihood of wear in different wheel/rail contact conditions. In combination with data from dynamic simulations, the wear data can also be used in prediction tools for comparison with other materials and contact conditions. Currently there is a lot of data available for standard grade materials [2], but not so much on premium grades, making the prediction of their performance in the field difficult.

In this work the wear performance of four premium rail grades against R8 wheel material was measured in a laboratory environment. Twin disc testing was performed using the SUROS (Sheffield University ROlling Sliding) machine. Material loss from wheel and rail discs was measured as well as friction in order to document the relationship of wear to $T\gamma/A$ curves. Conditions for testing were constant, with the exception of slip, which enabled variation of $T\gamma/A$ so that a benchmark wear map for a range of slip ratios could be established. Not all premium rail grades can be disclosed for this publication so rather than results specific to individual steels we focus on higher level conclusions relevant to premium grades in comparison to standard grade. The premium materials are referred to as R350HT, A, B and C. Comparison with R260 rail material laser clad with a layer of MSS from [4] was made as a further benchmark.

Standard rail material R260 is the basis against which the premium material is compared. R260 and one of the premium materials (R350HT) are designed in accordance with EN 13674-1:2011+A1:2017, which specifies Vignole rails of 46kg/m linear mass and with a hardness range of 200-440HBW. The rest of the premium materials are based on the manufacturers' own standard. All premium materials in this study are designed for 40-60kg/m linear mass for conventional and high speed railway track. Material R350HT has mainly wear resistant properties and it is designed for use on curved and heavy haul tracks. Material A is designed to be wear and RCF resistant in comparison to similar steel grade, commonly used in curved track and high duty areas, while material B is designed to be the most wear resistant grade with exceptional resistance to RCF, aimed for tightly curved and heavy haul tracks. Material C is mainly designed for RCF resistance and for use in critical areas such as switch blades.

2. BACKGROUND

Rail steel comes in many grades which have been developed over the years by the industry, aiming at achieving certain properties on the head of the rail where the contact with the wheel is taking place. Rail steel grades are normally categorised by the head hardness where in most cases the grade naming designation contains the minimum hardness value in Brinell. Premium rails are made with a target to increase wear resistance or RCF resistance or both.

However, there is a trade-off between these two properties as they are competing with each other depending on the operating conditions. Wear is the predominant damage mechanism that exists at different levels, in most loading cases and conditions. Rolling contact fatigue on the other hand only initiates when the cyclic loading level exceeds the material fatigue limit. This is when individual loading cycles have resulted in accumulation of plastic strain to the point that the material's resistance to further plastic strain is exhausted. At low $T\gamma/A$ values the most likely failure mechanism is RCF crack initiation and growth which at its worst, if unchecked, could lead to cracks turning down and causing a rail break. As the $T\gamma/A$ value increases, the wear rate in the system rises which removes material from the surface, thus removing any RCF cracks that may have initiated. At high $T\gamma/A$ failure will be by wear which is less catastrophic. This is encapsulated in the Whole Life Rail Model [5] that looks at wear and RCF interactions for standard grade rail. A $T\gamma$ damage curve is utilised that was developed based on field data and twin disc laboratory measurements. Hiensch and Steenbergen recently extended this type of approach to map this behaviour for other rail grades. This is limited in its application though as the same wear rate was assumed for all materials, which further emphasises the point made earlier about a lack of wear data for premium rail materials [6].

Some data is available though. Studies to characterise the wear and RCF behaviour of pearlitic and bainitic rail steels have been made by Stock and Pippan [7, 8]. The results indicated a reduction in wear, plastic deformation and the formation and growth of head checks (RCF) with increasing hardness and strength of five pearlitic rail steels, which were tested in a laboratory full-scale rig and also compared to track data. With regards to bainitic rail, tests indicated a lower wear resistance than the high hardness pearlitic rails, however, the potential of an improved RCF resistance was highlighted [8].

Past studies investigated the wear and RCF performance of rail materials for limited contact conditions, such as contact pressure (900-1,500MPa) or low slip ratio (creep) of around 0-6% [9, 10]. Bolton and Clayton tested at higher slip ratios but with lower contact pressure of 1,300MPa [11]. Under such conditions the mechanical energy that dissipates in the wheel-rail contact patch is not representative of the overall mix of loads that exist in the field. Heavy haul trains and multiple size wheels made of different steel grades affect the contact patch but also the environmental conditions, track geometry, friction modifiers as well as the driving behaviour of train drivers leads to increasing slip between the wheel and rail. Such increase in slip takes place at certain sections of the track, at tight curves or in braking and accelerating sections, and repetitive occurrence can be damaging for both the rail and wheel. As part of this study the contact pressure was maintained constant, but the slip ratios were tested at 1% as well as 10% and 20%. This caused an increase in the $T\gamma/A$ value and allowed direct comparison to damaging conditions that occur in the field.

Some of the issues with testing at the same contact conditions at small scale is the dissipation of heat generated. In the field the large mass of the wheel and rail aids in dissipating heat, in combination with the airflow around the system while the train is moving. To compensate for this in the twin-disc tests, compressed air was supplied to each wheel to aid in dissipating heat but also the duration of the tests was kept short with increasing slip, for example 10,000 cycles for 10% and 1,000 cycles for 20%. In addition, the compressed air was a way of removing the generated debris from the test machine, ensuring that the debris was not sticking to the discs.

The main characteristic of premium rail grades is their increased hardness, for example the higher the rail head hardness the more hard wearing the rail is expected to be. Hardness mapping was obtained in this study for the purpose of identifying the hardness variations in the premium rail as opposed to R260, and how this variation is represented in the twin disc specimens. Standard rail, for example R260, work hardens in the field and can eventually achieve similar surface hardness as some premium rail. That does not mean that it will perform the same as premium rail or rail with higher hardness, in terms of wear or RCF resistance and this can be seen from this comparable study. Superficial hardness may not be as effective as through thickness hardness, since it can be re-worked during operation and the rail head may experience multiple phases of plastic deformation, ratchetting and hardness fluctuations in comparison to materials designed for high wear resistance. Other methods to increase the hardness/wear resistant properties of the rail head is with the use of laser cladding. These methods are of interest due to the thicker coatings that can be produced in relation to more traditional coating techniques (μm versus mm). Figure 1a is a hardness profile of R260 material, the four premium materials and a laser clad R260 with a coating of MSS steel of a 1mm depth. The hardness measurements were taken after the samples were tested at 1% slip for 30,000 cycles from the edge of the disc contact surface in a linear trajectory towards the centre of the disc up to 2mm into the depth of the material. It is clear that all materials have had some sort of work hardening, affecting the material at about 300μm below the surface while the R260 material has had a much greater hardness change of all of them to a depth of about 800μm.

In comparison to the MSS Clad it can be observed that the higher hardness of the clad material runs to a depth of just over

1mm from the surface and this highlights the possible benefits of using thicker coatings. Area hardness measurement of the MSS Clad sample was conducted with 33 indentations. The resultant hardness map is shown in figure 1b, where the top of the figure is the area closer to the edge of the SUROS disc. Figure 1c is the three-dimensional representation of figure 1b. There is a characteristic upwards and then downwards spike in the dilution zone, which is highlighted in figure 1c.
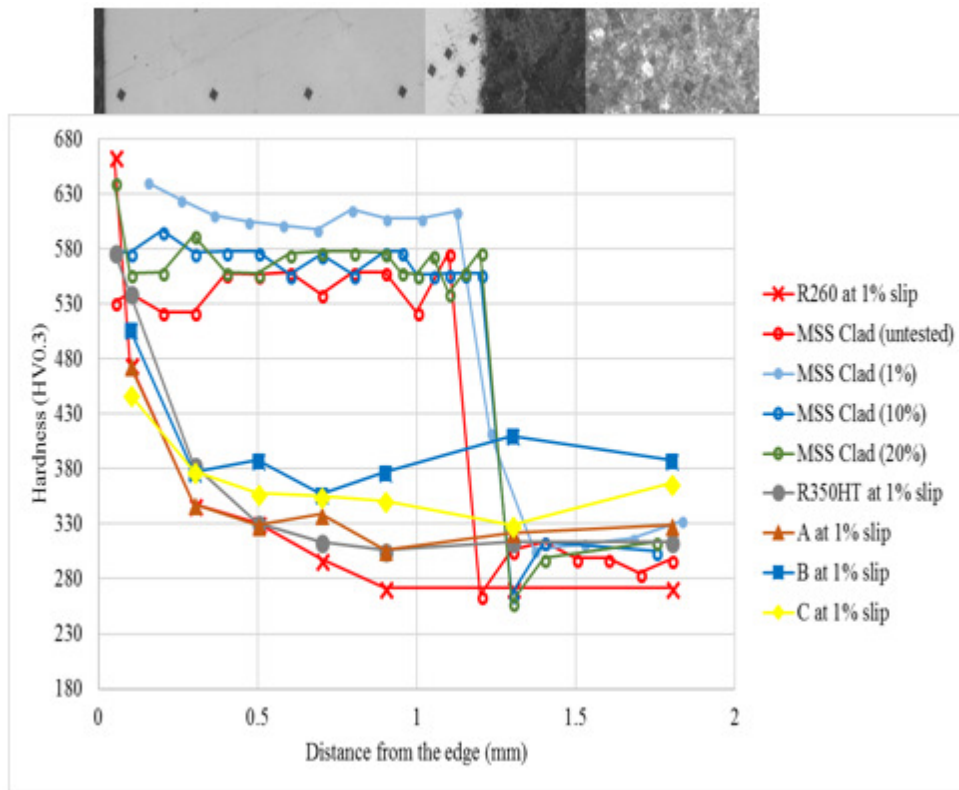

Figure 1a *Hardness profile through the thickness of sectioned samples and stitched image of untested MSS Clad (using Struers DuraScan at HV0.3).*

Max=689Hv Min=268Hv Range=421Hv Mean=474Hv Ind=33 St.Dev=131.9528
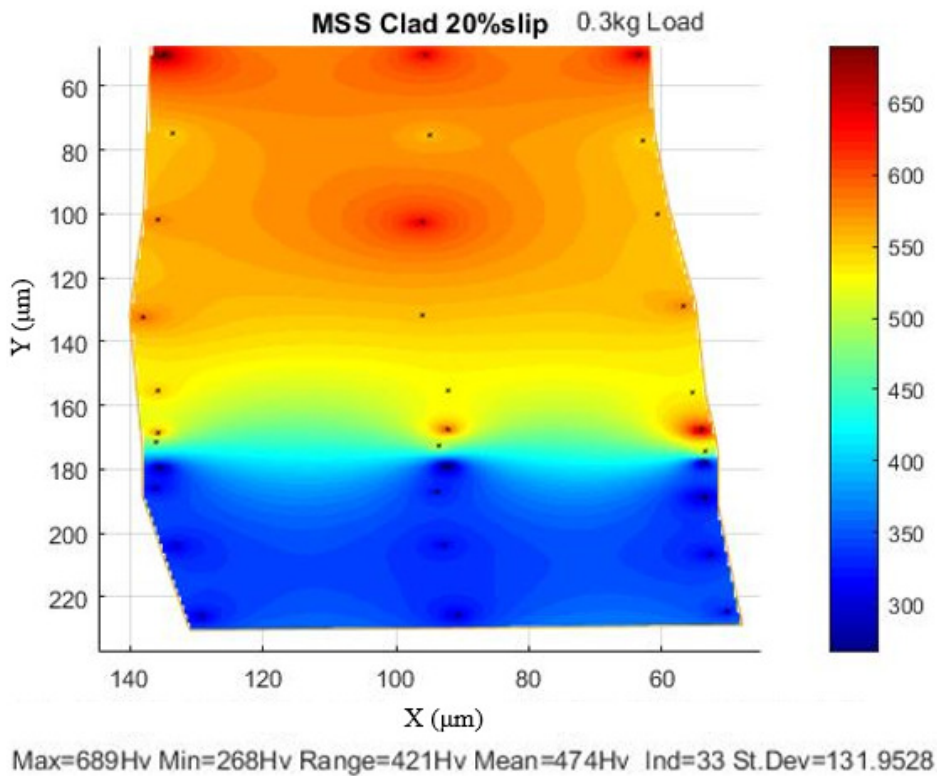
Figure 1b *Hardness mapping of the through the thickness of sectioned MSS Clad sample (using Struers DuraScan at HV0.3). Dimensions in μm, where the top of the graph is the edge of the SUROS disc.*
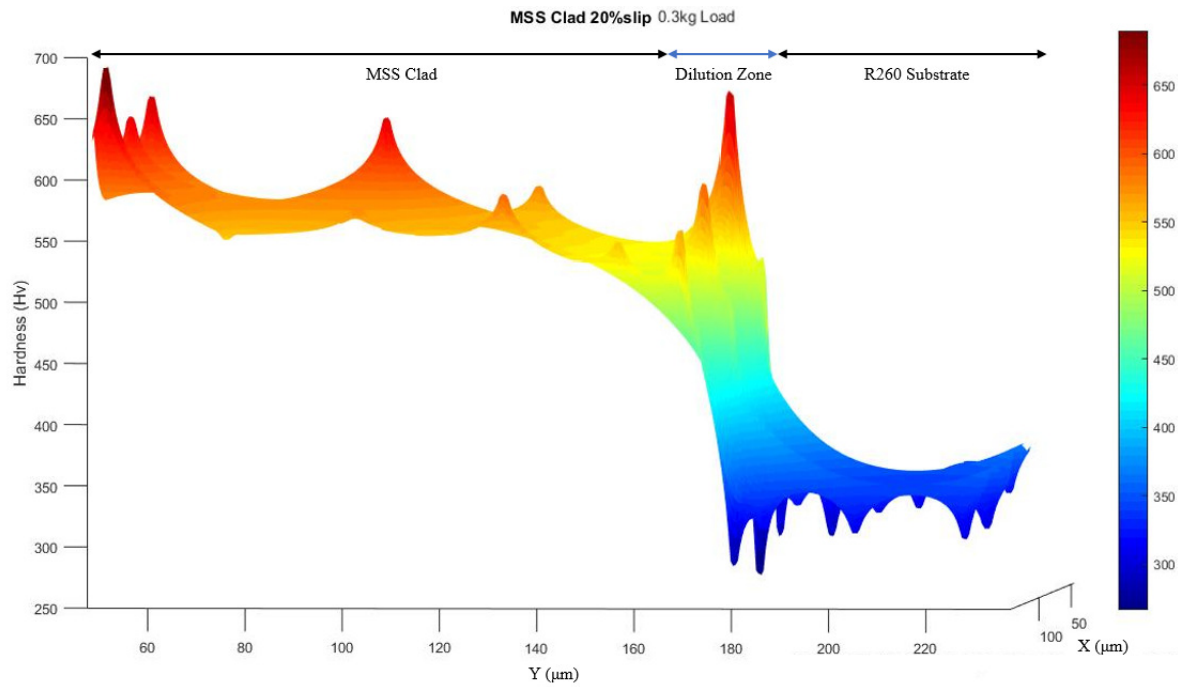
MSS Clad 20%slip 0.3kg Load

Figure 1c Hardness mapping in 3D view of figure 1b. The characteristic spike upwards and downwards in the dilution zone is prevalent in the hardness mapping as first indicated by the hardness line profile in figure 1a . Horizontal axis in μm, vertical axis in Hv0.3.

The laser clad material is a form of Martensitic Stainless Steel. A chemical analysis was obtained using an optical emission spectroscopy method on the surface of the disc, which indicated the quantities of elements as listed in table 1.

C [%]	Si [%]	Mn [%]	S [%]	P [%]	Cu [%]	Ni [%]	Cr [%]	Mo [%]	V [%]	Co [%]	W [%]	Balance [%]
0.22	0.18	0.87	<0.003	0.011	<0.01	2.25	9.53	0.24	0.27	1.22	0.46	84.75

Table 1 Chemical analysis of the R260 laser clad disc

3. MATERIALS AND TEST METHOD

Laboratory tests were the preferred method of evaluating the wear performance of the premium rails because it is an economical way which allows to obtain results much quicker than in the field. In addition, the use of a small scale twin-disc tester allows for replication of the tests under the same conditions, which can be difficult to achieve with field trials. Tests were planned in line with the good practice as described by Lewis et al. [4]. The SUROS twin disc machine [4] (see figure 2) was set-up at a maximum Hertzian contact pressure of 1500MPa and a rail disc rotational speed of 400rpm. The slip between the wheel and the rail discs was controlled by increasing the wheel disc rotational speed by the appropriate percentage of 1%, 10% and 20% of the rail disc's rotational speed, thereby representing a driving wheel. A torque transducer positioned on the rail disc drive shaft was used to measure torque and enabled calculation of the tractive force and therefore the $T\gamma$ for each test. Tests were performed in dry conditions for varying numbers of cycles (1,000 cycles for 20% and up to 30,000 cycles for 1% slip). The discs have a contact width of 10mm and a diameter of 47mm (see figure 3a). The room temperature was varied between 22°C-28°C and the humidity in the room between 30%-60%.
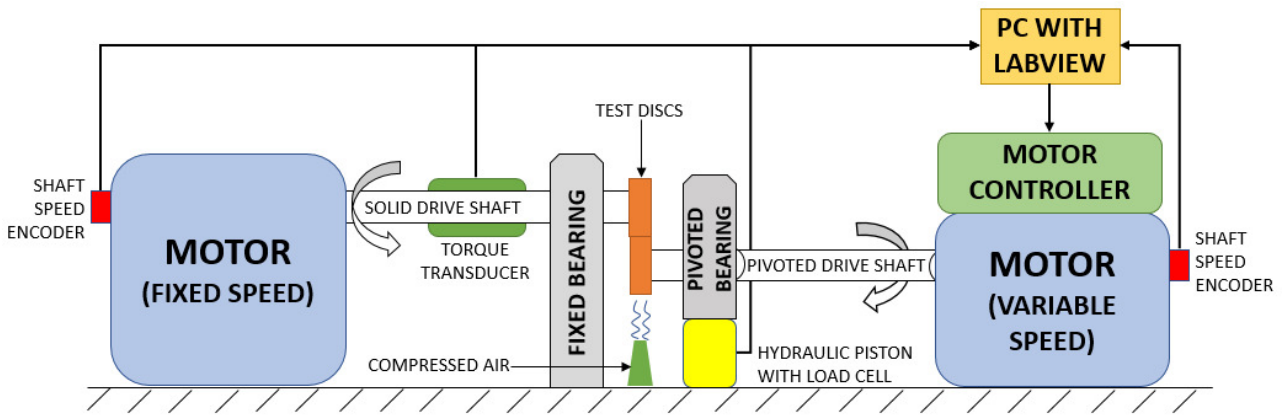
Figure 2 Schematic diagram of the SUROS twin disc testing machine

The specimens were cut from the rail head of each material and machined into SUROS discs. The hardness in each rail head may vary, since some premium rail grades are designed to have an increasing hardness towards the rail head. Also, due to inconsistencies in the manufacturing process, the hardness may vary in different parts of the rail head and through the thickness of the standard rail. This means that the hardness of the disc samples may vary slightly around the contacting face with the opposing disc (wheel). Similarly, the wheel was machined from the outer rim of an R8 wheel which complies with BS 5892:3. Typically such wheels have a harder running face which is softer towards the centre of the wheel. The samples used for the test were taken at random from different batches, tested in no particular order and the tests took place over a ten-month period.

Before commencing a test, the specimen discs were dipped in acetone and cleaned in an ultrasonic bath for two minutes. The weight of each disc was recorded using the Adam AAA-300L weighing balance with an output of four decimal points (0.1mg precision). For the 1% slip, the test was interrupted every 5k cycles up to 30k, in order to record the wear of each disc. Before measuring the wear, the discs were cleaned again in ultrasonic bath as at the beginning of the test. For the 10% slip, the test was interrupted at 1k, 2k, 3k, 4k and 10k cycles. Finally, for the 20% slip, the test was interrupted at 500 cycles and 1k cycles.

After the tests were completed, the discs were sectioned in three cutting planes in order to expose an internal face of the disc in the middle of the outer rim (see figure 3b). The sectioned pieces were mounted and polished for further analysis including hardness testing. Micro-hardness testing took place with a load of 0.3kg in multiple locations from the outer rim of the disc towards the centre in the section in order to observe any work hardening effects occurring near the running area of the disc (figure 1a). Surface images were also taken.
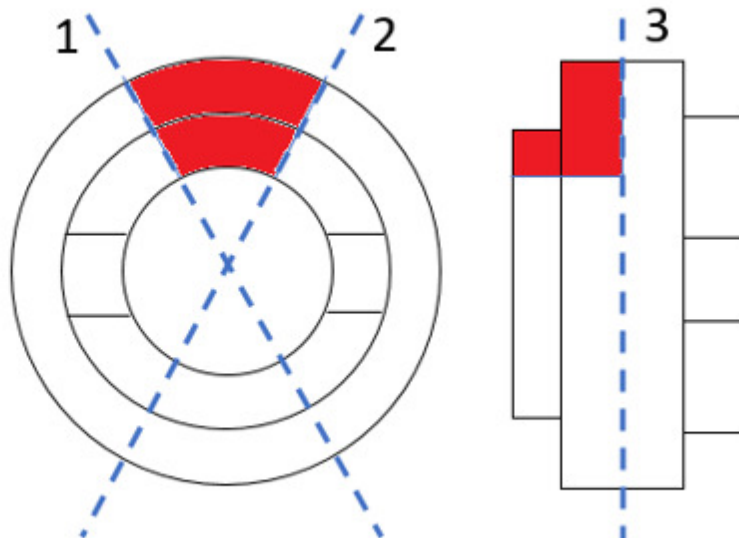

Figure 3 (a) Image of test discs mounted on the SUROS tester.   *(b) Locations of the three section cuts (sample highlighted in red).*

4. RESULTS

The results are presented in terms of wear rate for the rail (figures 4) and for the wheel (figure 5). In terms of wear rate over $T\gamma/A$ for the rail (figure 6) and lastly in terms of system wear which includes the wheel and rail (figure 7). In figure 4 the wear rates are represented for the three slip ratios tested, split into three graphs. For the 1% slip the measurements taken every 5,000 cycles up to 30,000 cycles. This test approach was adopted from [2] and used to monitor the wear evolution of the different materials.

In the same graph data from other tests of laser clad rail performed under the same conditions [12] have been added (MSS Clad) for comparison with the R260 baseline and premium materials. For calculating the wear rate for the 10% and 20% tests, the overall mass loss was divided by the number of overall cycles to produce a wear rate figure of mass loss per cycle while for the 1% slip tests, only the mass loss in the last 5,000 cycles was used for calculating the wear rate, since it takes about 20-25,000 cycles for the wear rate to reach steady state when testing at 1%.
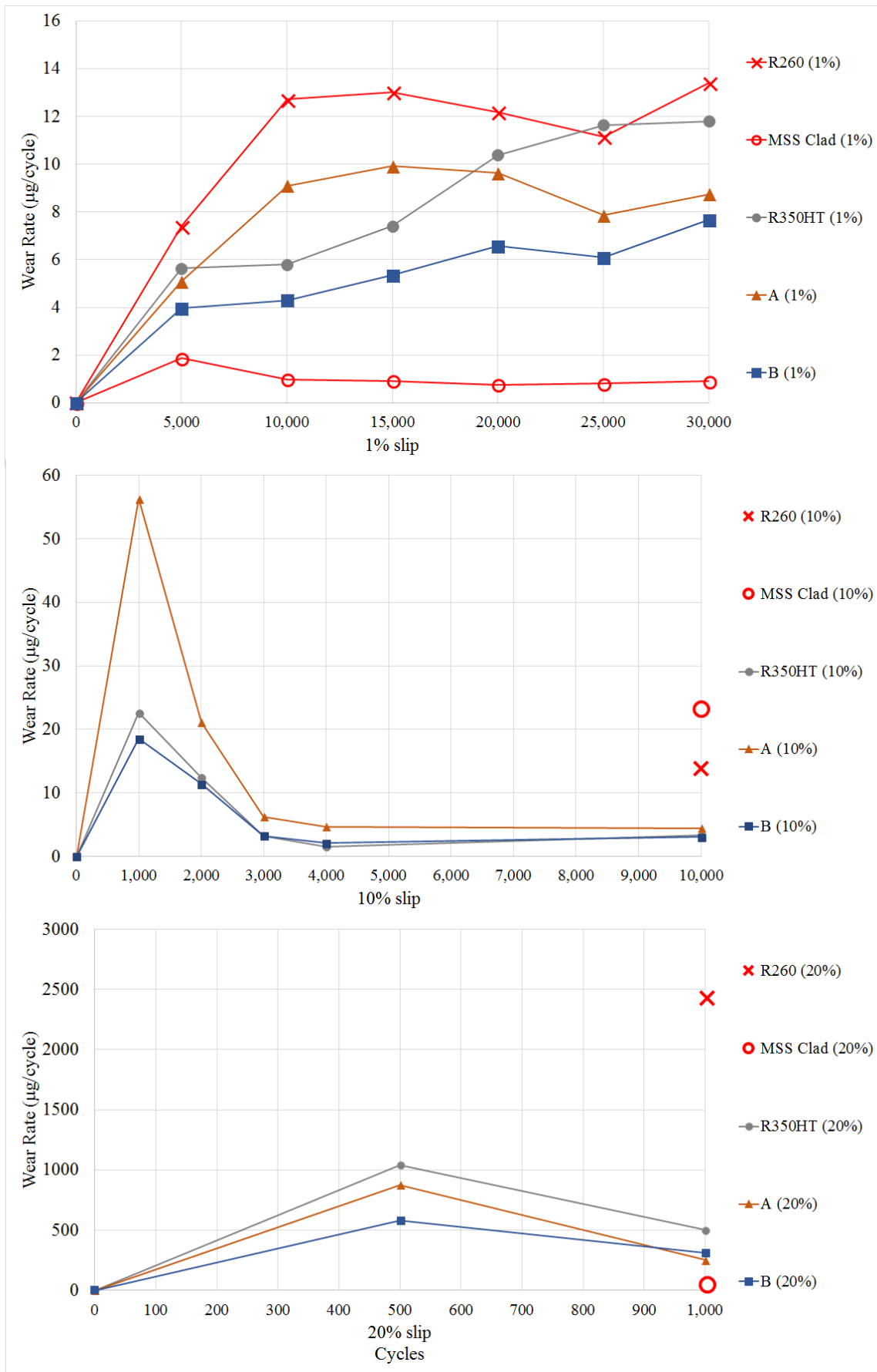
Figure 4 *Rail wear rate per cycle at 1%, 10% and 20% with 1500MPa contact pressure and 400 rpm primary rotational speed.*
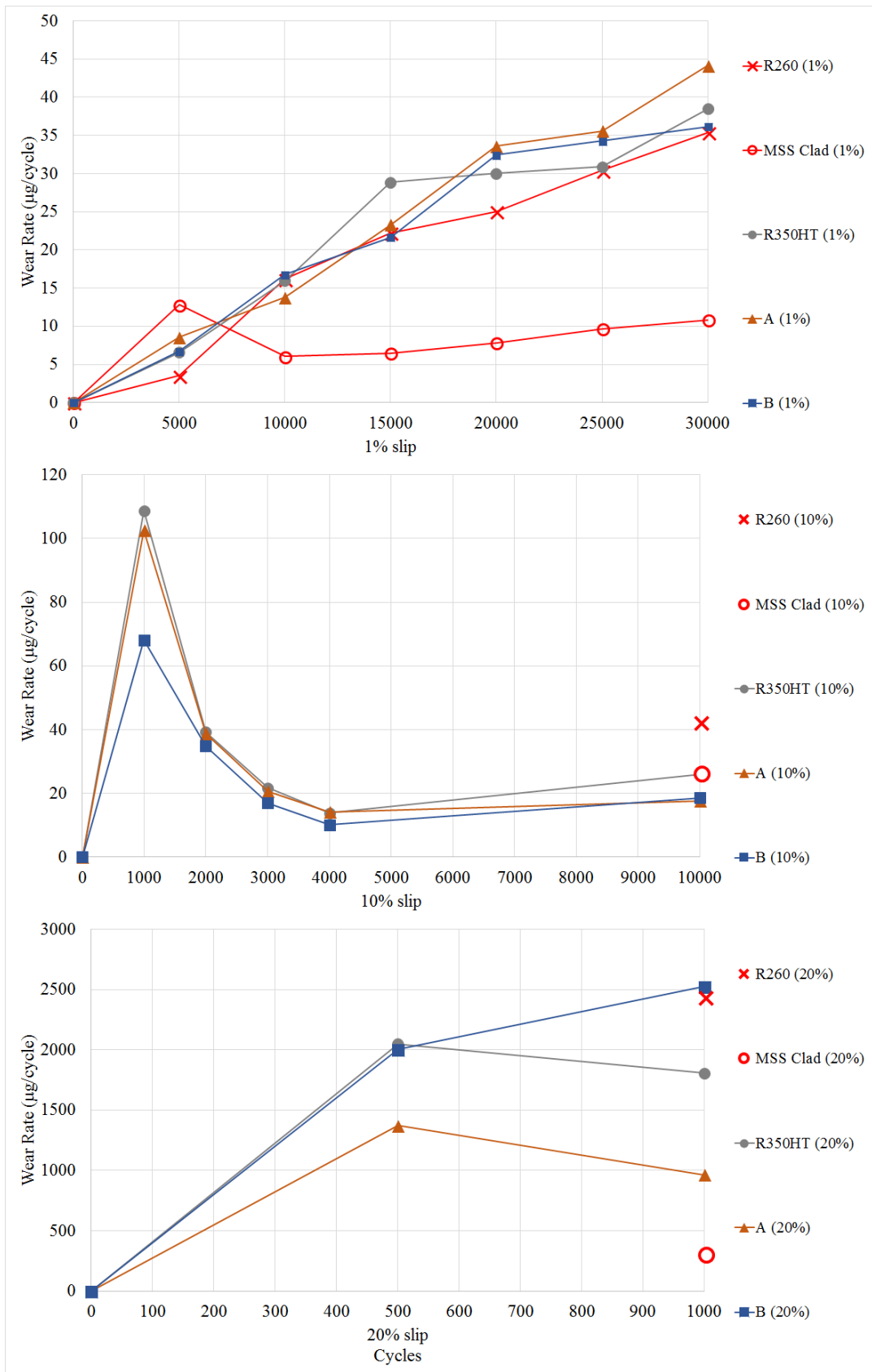
Figure 5 *Wheel wear rate per cycle at 1%, 10% and 20% with 1500MPa contact pressure and 400 rpm primary rotational speed.*

In some repeat tests the wear rate was only measured at the beginning and at the end of the test, so it was preferable to indicate the overall wear rate for comparison, including a "run in" period. The "run in" period varies depending on the material and slip ratio.

Material C showed poor wear resistance in comparison to the other materials at 1% and an extremely high wear at 10% and 20%. In addition, the shape of the material C disc has turned from cylindrical into a polygonal shape, while the wheel disc has remained cylindrical. Material C is aimed at improved RCF resistance rather than improved wear resistance and it is difficult to say why the rail disc has taken this form without further investigation and testing. For this reason, the results for material C for 10% and 20% have been omitted from the graphs in this section.

Figure 6 is put together using the calculations from equation 1 and equation 2, where the contact energy over 1mm^2 area ($T\gamma/A$) is plotted against the wear rate (μg/m/mm^2). The data points are forming three distinct areas on the graph, which resemble the three wear regimes of "Type I-Mild", "Type II-Severe" and "Type III-Catastrophic" [2, 11, 13]. A Schematic of this typical relationship of pearlitic steel indicating a predicted path for the data points is shown in figure 17. This path on the graph is verified in figure 6 and highlighted with the exception of material C.
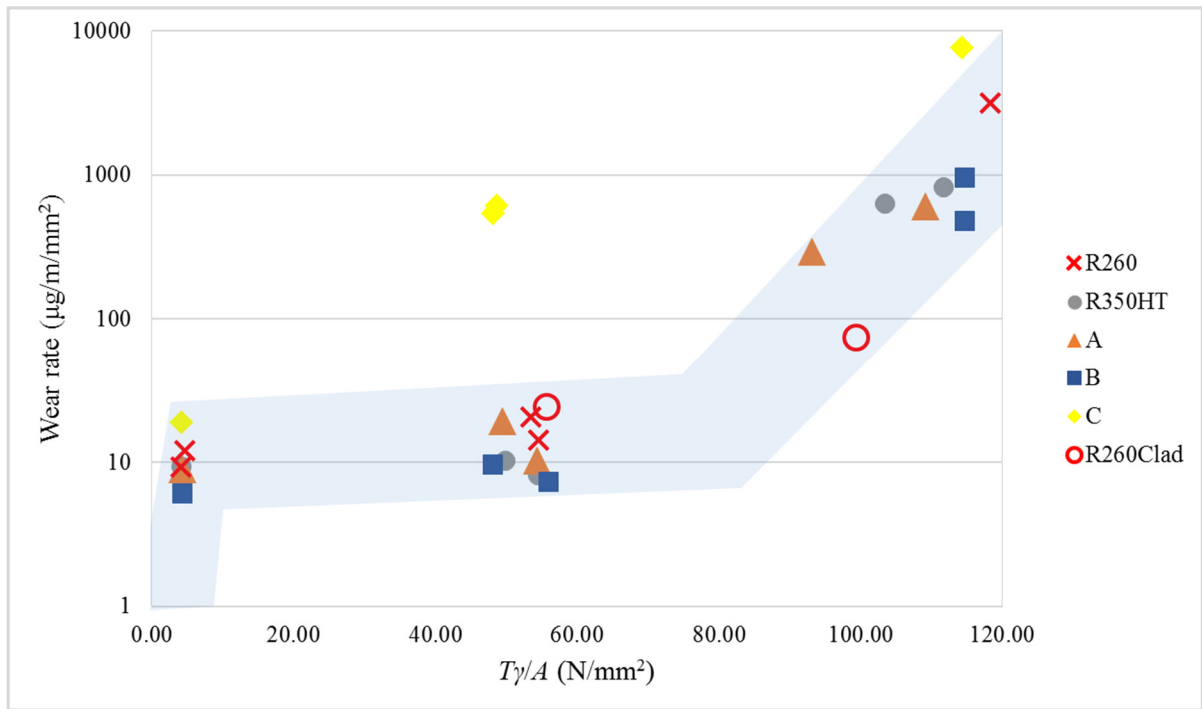

Figure 6 Rail wear rate vs Tγ/A.

A way to describe how much wear damage is attributed to the wheel and how much to the rail, figure 7 was put together. The overall wear in μg for the wheel and rail is shown in for each slip condition, with the exception of material C.
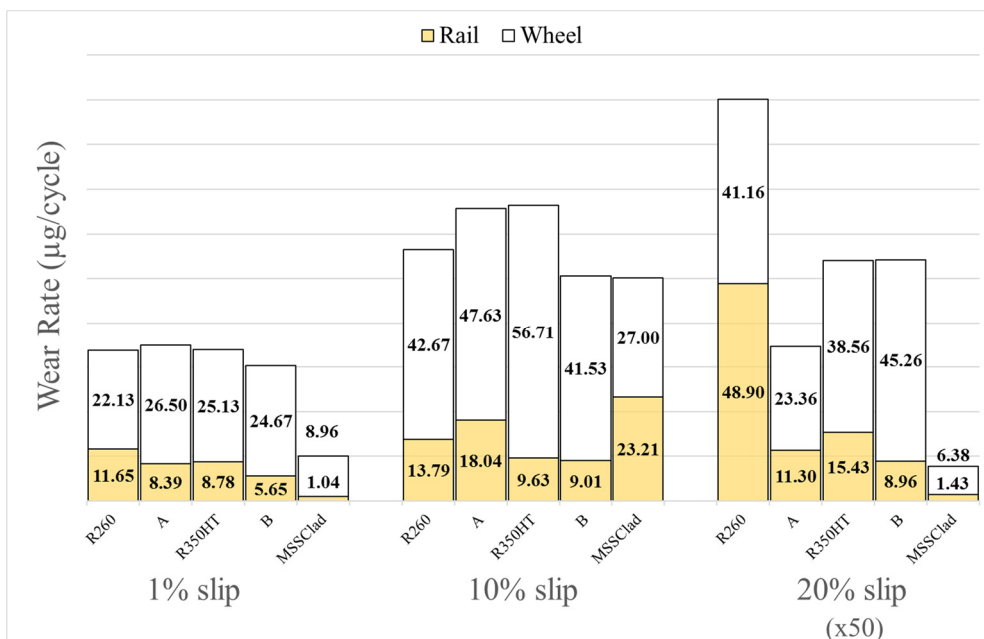

Figure 7 Cumulative System wear (20% is shown on a different scale).

9

Etched images from an optical microscope are shown in figures 8-12 with a 5x objective lens magnification. In some images the hardness diamond indentation is still visible after etching. The rolling direction indicates the direction the axis of the disc would be displaced, if the opposing disc was a flat surface.
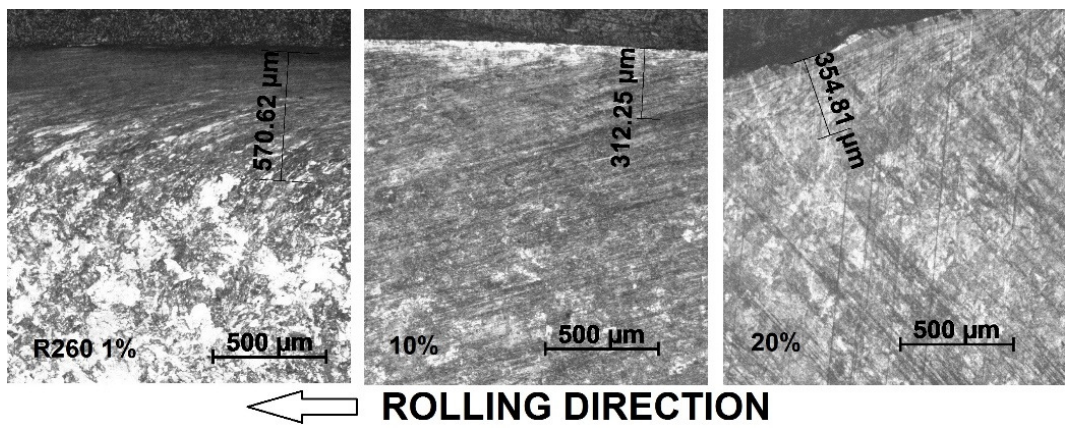

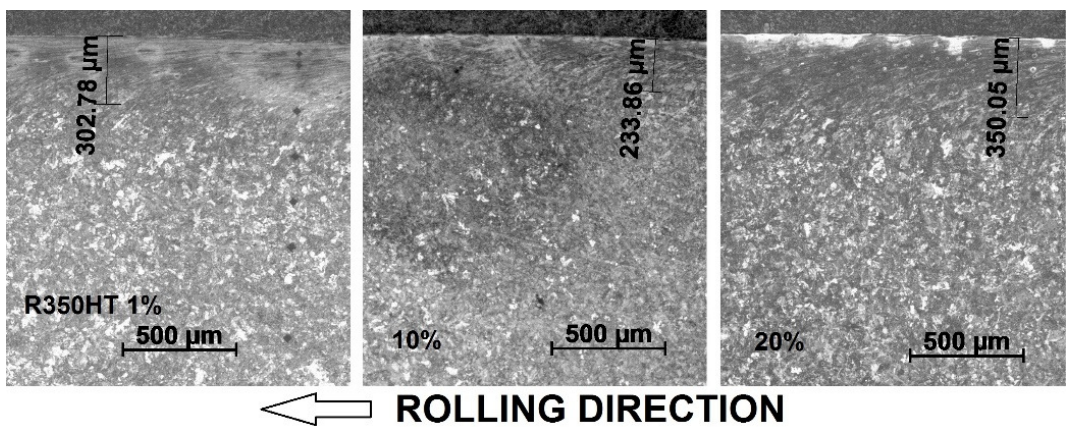*Figure 8* Optical microscope images of R260 (1%, 10%, 20% slip).

Figure 9 Optical microscope images of R350HT (1%, 10%, 20% slip).
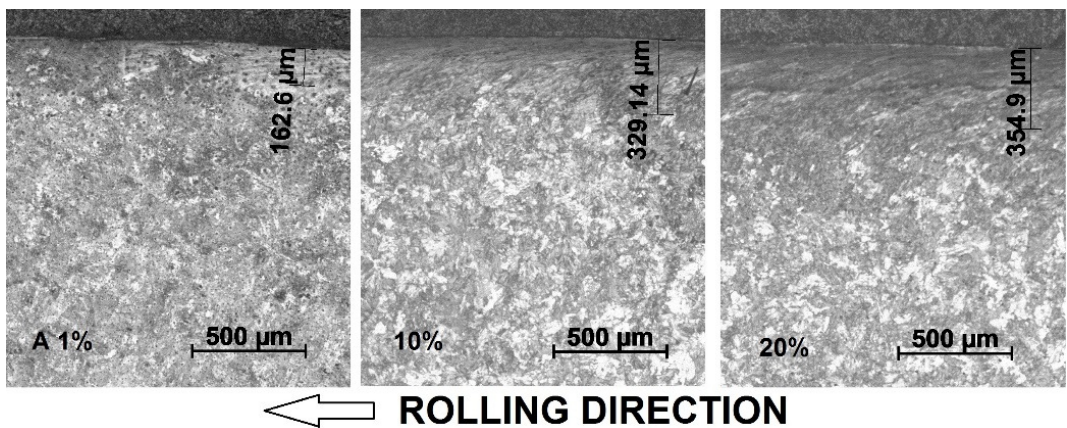

Figure 10 Optical microscope images of A (1%, 10%, 20% slip).
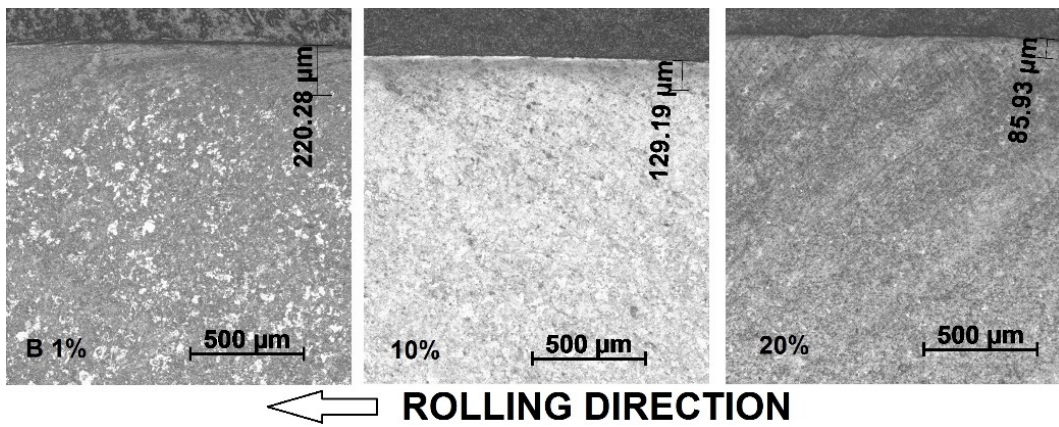
Figure 11 Optical microscope images of B (1%, 10%, 20% slip).
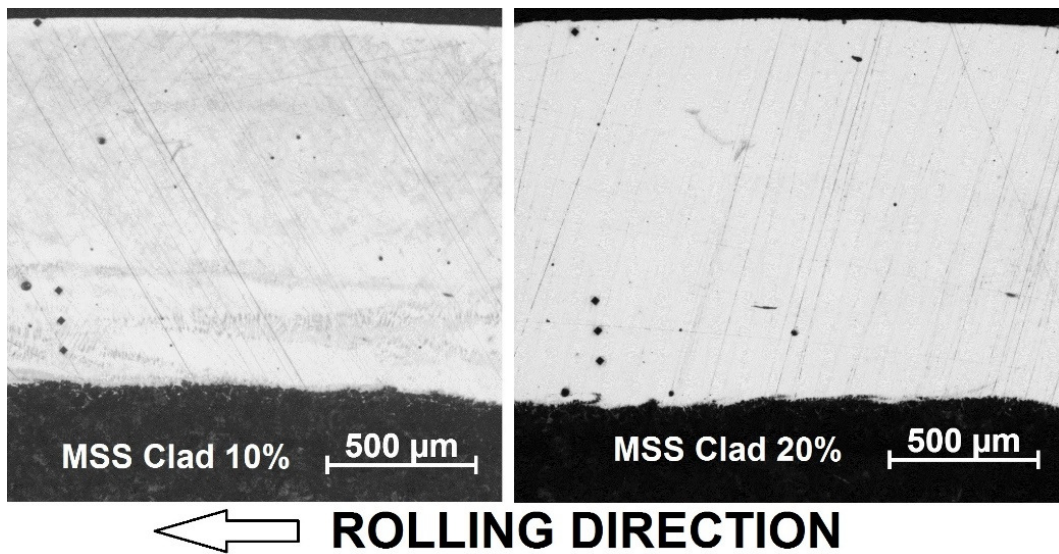
Figure 12 Optical microscope images of material R260 with MSS clad, from 10% and 20% slip etched samples - Very small plastic deformation.

Finally figure 13 shows pairs of rail and wheel discs for the 20% slip test, while figure 14 shows images of the etched samples taken from the 20% slip test of the R8 wheel material. The notation on the images indicates the rail discs material reference, R260, R350HT, A and B. There is a peculiar phenomenon of plastic deformation which differs in each material combination and rolling conditions.

Figure 13 *Image of wheel and rail discs after testing at 20% slip.*
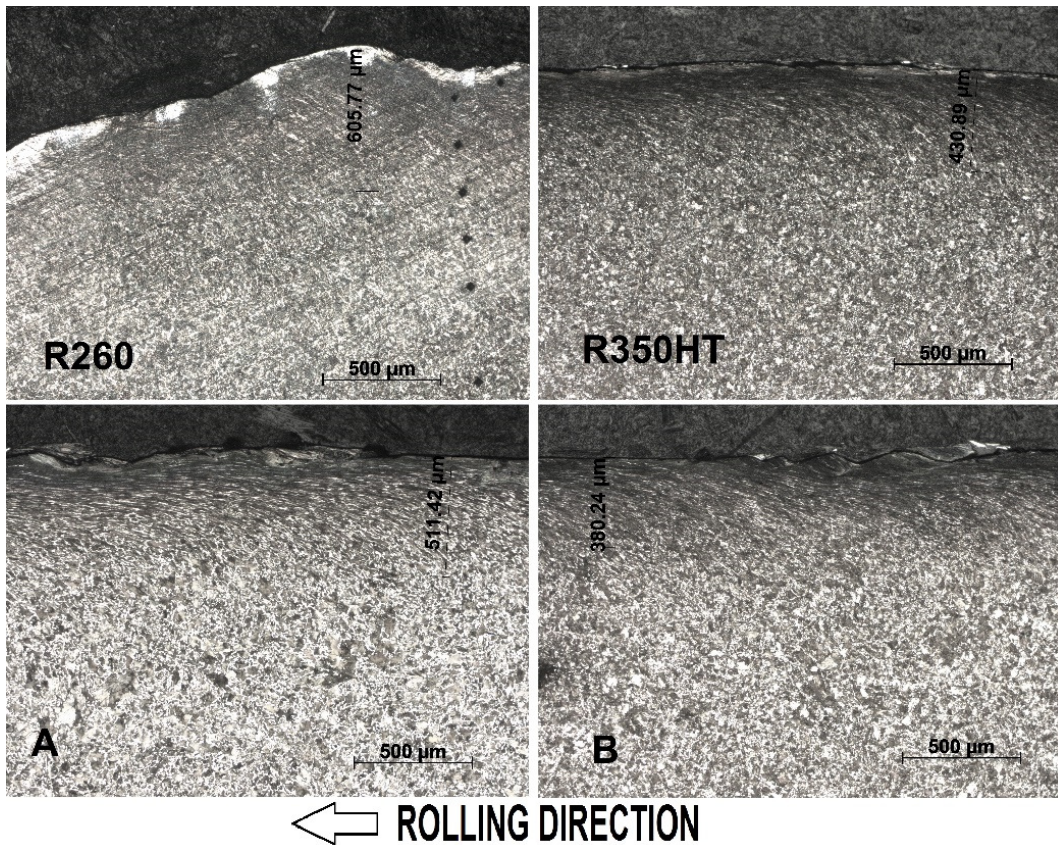
Figure 14 *Optical microscope images of wheel material R8, rolled against R260, R350HT, A and B rail discs, taken from 20% slip etched samples.*

For the material A test, the wheel exhibits short flat areas which did not form on the rail material. This is similar to the material B tests, where the rail has been plastically formed into a polygonal shape, while the wheel has remained round. In magnification the plastic deformation near the surface exhibits a wave pattern, as shown in figure 15.

Figure 15 *Image of wheel disc (Material B-tested at 20% slip) indicating the waviness of plastic deformation near the surface.*

For the material R350HT test, the wear patterns on both the wheel and rail are similar to the lower slip tests while for the material C test extreme wear and plastic damage is shown on both the wheel and rail. The R260 test has shown another peculiar phenomenon where both the wh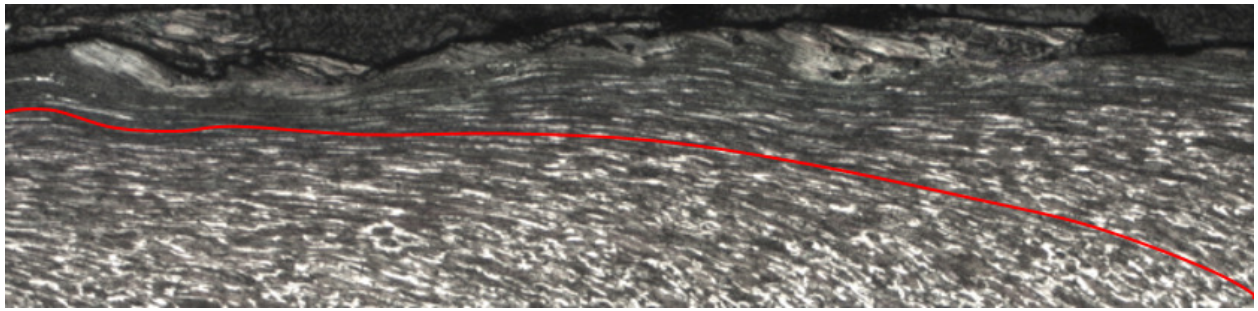eel and rail discs have formed a matching pattern between them that resembles a helical gear. This is visible in figure 13, where the edge of the disc is sloping and where material has been removed as well as plastically deformed. This phenomenon could be induced by many things such as high temperatures in the contact zone and the plastic deformation attributed to the work hardening properties of R260.

Hardness mapping was performed using a Struers Durascan micro hardness machine. Cylindrical off cuts of the SUROS discs were ground and polished. Railhead specimens of the premium materials were cut from unused rail with an Electrical Discharge Machine (EDM) which is a slow process that induces small localised heat and plasticity to the sample, which is easily removed by grinding, as opposed to other cutting methods. Parallel slices of 20mm in thickness were obtained. The indentations were taken at random on the surface of all samples at a macro level of 3kgf load. The load duration varied according to the Ecos Workflow™ software which determines the duration of each indent based on a number of parameters and the results were exported in a spreadsheet for further analysis using Matlab. A code was developed based on the code described by Brayshaw et al. [14] where an interpolation method is used between the indentation datapoints and a surface plot is created. Outside the datapoints boundary, the values are normalised to the average hardness value of the dataset and the final plot is trimmed around the boundary. Due to the difficulty in obtaining hardness results very close to the boundary, indentations were obtained about 0.5-1mm from the boundary. When plotting the results the boundary has been offset by a small amount to represent the true boundary of the specimen. Bearing this in mind, the hardness maps shown here are macro scale maps and do not represent the true hardness at the very edge of the specimen or the true boundary geometry, but a very close approximation.

Figure 16a *Hardness mapping on the surface of material R260 Rail and SUROS disc specimens*

R350HT Railhead — Max=380Hv Min=264Hv Range=116Hv Mean=350Hv Ind=241 St.Dev=17.3053

R350HT SUROS — Max=370Hv Min=275Hv Range=95Hv Mean=338Hv Ind=42 St.Dev=21.6916

Figure 16b *Hardness mapping on the surface of material R350HT Rail and SUROS disc specimens*

A Railhead — Max=386Hv Min=302Hv Range=84Hv Mean=340Hv Ind=413 St.Dev=15.0664

A SUROS — Max=393Hv Min=278Hv Range=115Hv Mean=334Hv Ind=47 St.Dev=19.7155

Figure 16c *Hardness mapping on the surface of material A Rail and SUROS disc specimens*

B Railhead — Max=434Hv Min=314Hv Range=120Hv Mean=378Hv Ind=183 St.Dev=22.4951

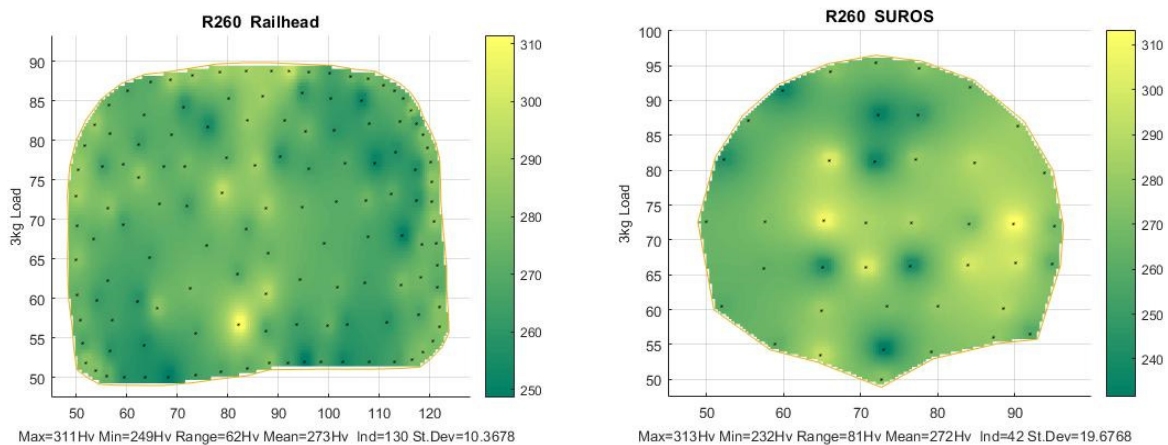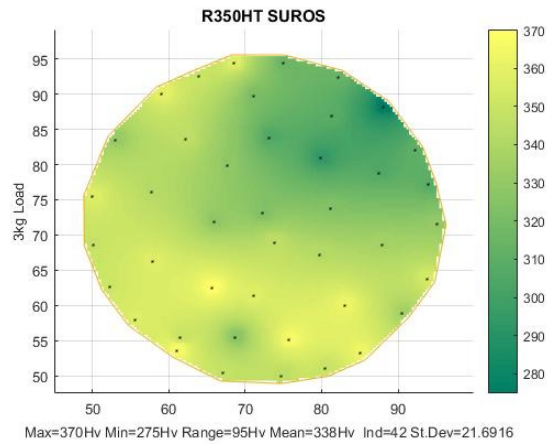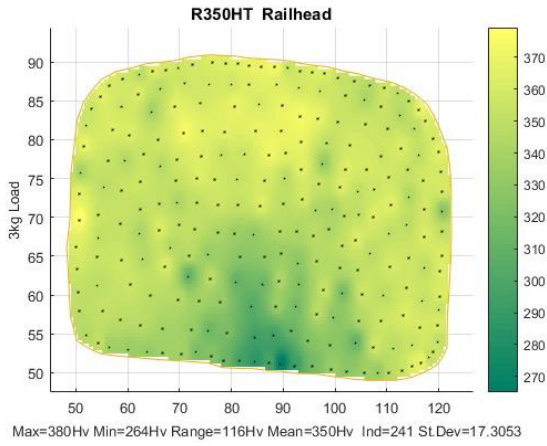B SUROS — Max=411Hv Min=306Hv Range=105Hv Mean=361Hv Ind=39 St.Dev=23.526
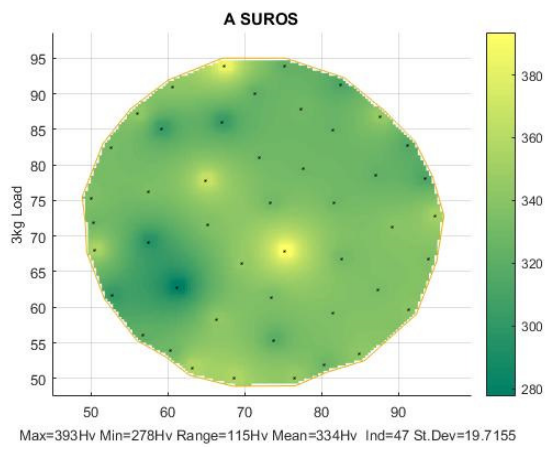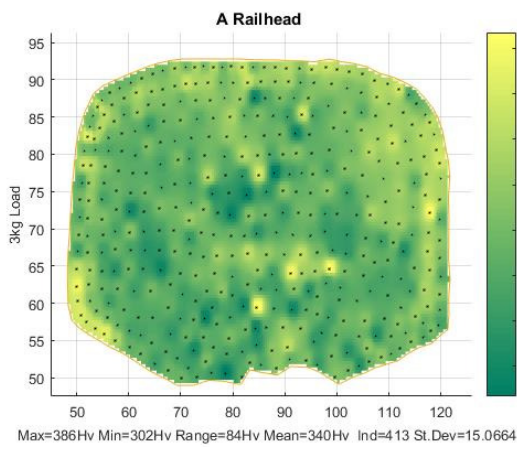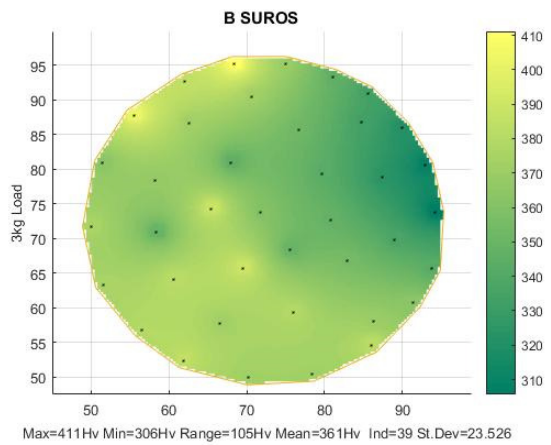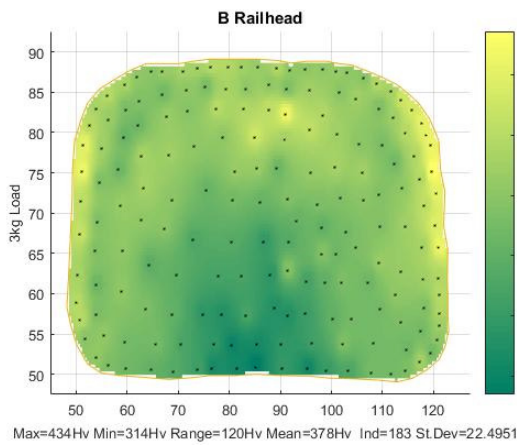
Figure 16d *Hardness mapping on the surface of material B Rail and SUROS disc specimens*
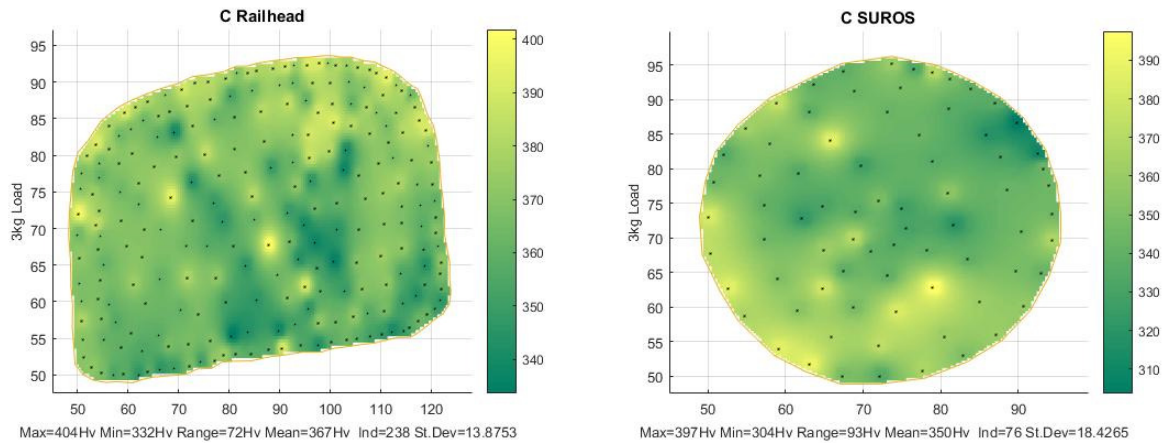
14

Figure 16e *Hardness mapping on the surface of material C Rail and SUROS disc specimens*

5. DISCUSSION

The rail wear rate for all materials at 1% slip, increases until a steady state is reached before 30k cycles, see figure 4, while for the laser clad material it decreases to a steady value. Blau [15] explains that the wearing behaviour during testing happens in stages, depending on the type of wear. Transitions from one stage to the next can be induced by external changes (Type 1) or they can occur naturally (Type 2), for example running-in, wear of coating and thermally-induced from the build-up of heat. An oxide layer on the surface of the specimens contributed to the initial running-in stage.

The measurement of the mass loss was made periodically and the frequency of stopping can be detrimental in capturing different stages. The initial measurement was made at 5,000 cycles (1%), 1,000 cycles (10%) and 500 cycles (20%). The initial stage, for example an incubation period before the wear-in period, followed by a sudden acceleration in wear was missed and two stages can be seen, of acceleration in wear and a terminal stage. For this reason, the wear data used for the calculation of $T\gamma/A$ are normalised. In some cases, for example at 10% slip, the wear rate generally starts at a high rate and decreases until it reaches a steady state at around 10k cycles. Four transition stages were captured here, the acceleration, maximum rate, deceleration and terminal stages. Similarly, at 20% slip the deceleration stage can be identified from the three data points, as it is decreasing between the 500 and 1,000 cycles data points. This clearly describes the extreme damage which is happening at higher slip and which wears the material at a higher rate until a steady state is reached as opposing to the low slip case where the wear rate is increasing slowly. Figure 5 is showing data for the wheel of the same material as tested against the different rails as shown in the legend. The wheel is behaving in a similar way, however, it seems that the wear rate at 1% has not reached a steady state, but it is still increasing. For the 10% and 20%, the change in wheel wear rate has a similar profile to the rail but at different levels.

Figure 6 is a typical representation of wear rate over $T\gamma/A$ and most data points seem to follow the observations of Lewis et al. [13] as explained in the previous section and described by figure 17. The wear rate is expected to increase with more traction in the interface and this is achieved with each increase of the slip ratio. Three groups can be observed, representing the 1%, 10% and 20% slip, each with a calculated $T\gamma/A$ value, with 1% at $T\gamma/A$ values below 10N/mm², 10% at values in the region of 50N/mm² and 20% at values over 90N/mm². The standard rail R260 showed the worst wear resistance at higher $T\gamma$ levels along with material C which was wearing significantly more in all slip cases and it is outside the expected wear zone, as highlighted in the graph. The R260 repeat test at 20% slip was omitted from this graph as the test was not comparable to the other data due to the large plastic deformation that cause the helical gear patterns as shown in figure 13. Due to this matching shape on both wheels, the friction in the system was increased to more than 0.5, resulting in high $T\gamma$ values outside of the scale of figure 6 and subsequent very high wear under non rolling sliding conditions.
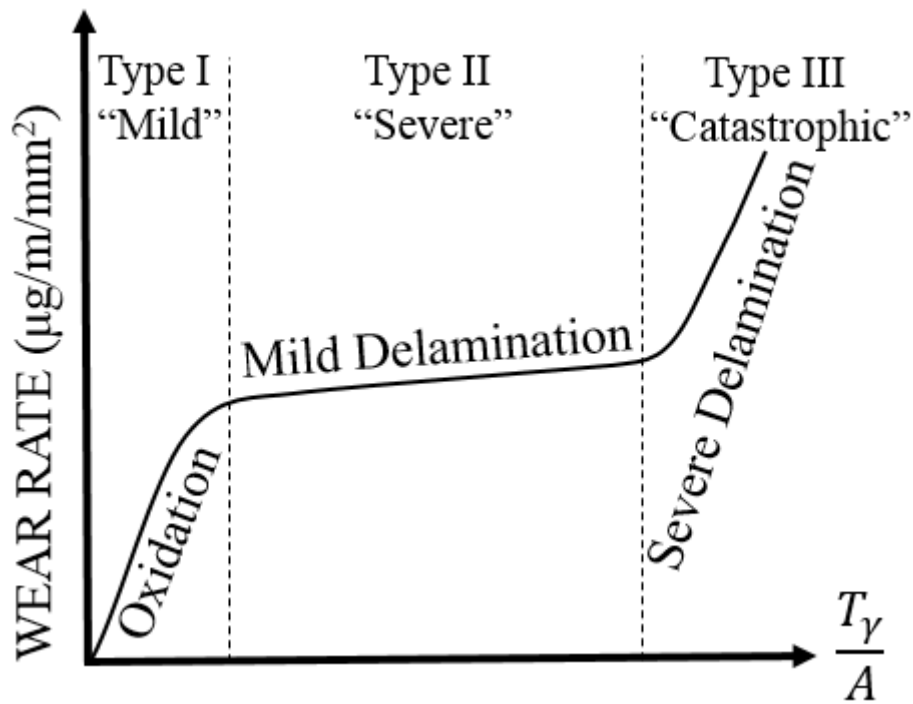
15

Figure 17 Schematic diagram of wear regimes (adapted from Lewis et al. [13]).

Materials A and R350HT are designed for wear resistance and they have a similar performance at all slip conditions. There is a difference in system wear though which indicates that at 20% slip material R350HT is wearing the wheel more than material A.

Material B is designed to be the most wear resistant grade and it seems to stand out as a lower wearing material in all cases. Even though the data points at 20% indicate higher wear, these are at much higher $T\gamma$, at harsher conditions. However, the system wear (figure 7) for material B is worse than the other materials at 20% and this is due to the wheel wearing more at high creepage. Material C is mainly designed for RCF resistance and during these tests it showed poor wear resistance with unwanted plastic deformation at all slip ratios and outside of the expected wear performance in comparison to the other rail materials. An R260 laser clad with MSS was tested to provide another point of reference of a non-commercial rail material. Although the laser clad material exhibits higher wear than the other rail materials at 10%, it is performing much better at 20% slip, with much lower wear than the other rail materials. However, in all cases for the laser clad material, the system wear is significantly low, and this is because the wheel is wearing less in all cases when the laser clad material is used. This observation highlights the importance of considering the wheel wear when comparing different rail materials and perhaps the selection of premium rail should be conducted as a system wear methodology.

The balance between rail wear and wheel wear varies for each material at 1% slip, and this can be seen in figure 7. The overall system wear is more or less the same for all materials with the exception of material B which is slightly lower and the laser clad material which is significantly lower. This is an indication, that despite the various materials with various hardness levels, the system is wearing in such a way that it always wears out the same amount for these set conditions, either from the wheel or the rail. It is only for material B and for the laser clad material that the system wear is reduced. Figure 7 illustrates that in both of these cases the wheel is wearing significantly more than the rail, but still the overall system wear is lower than the other cases.

The difference in wear between the different rail materials as well as the wheel materials is attributable to the intrinsic mechanical properties of the materials which are different since all the materials tested do not have the same chemical composition or post manufacture processing such as heat treatment. In some cases, for example at low slip, most of the premium materials behave similarly, while at high slip some of the material characteristics help reduce wear. From the initial test results it was observed that the wheel is wearing more than the rail in all slip cases. The difference in wear rate between wheel and rail is small at low slip ratio, for example at 1% slip it is in the region of 5μg/m/mm². For the 20% slip the difference in wear rate between wheel and rail has increased and it is in the region of 2000μg/m/mm².

To bring the amount of wear into perspective, let's assume that one of the wheels of a typical train has a contact patch area of 70mm² then if the rail was made of R260, for every km of rail that the wheel is passing, the rail would wear by 0.7g (10μg/m/mm² at 1% slip, and around 4N/mm²-$T\gamma/A$), while if the rail was made of material B it would wear by 0.42g (6μg/m/mm² at same conditions) and this is calculated by multiplying by 1,000 metres and by the square patch. From this comparison we can see that if this particular kilometre of R260 rail was to be replaced by material B, it would probably

increase the service life by 40%. In reality the overall traffic must be calculated for different sections of railway, so the wear rate must be multiplied by the number of wheels for each train and the number of trains that will run over a certain period of time based on a schedule. It is more complicated to estimate total rail wear as the traffic and rolling conditions change continuously, so the results from this study can only be used for direct comparison between the different materials, unless they can be used with more sophisticated simulation and prediction software.

Hardness mapping of railhead and SUROS specimens was conducted at macro level (3kgf load) in order to compare the hardness profile of the twin disc specimens with the railhead hardness profile. The twin disc were manufactured from the middle part of the railhead. The hardness indentation duration was around 40 minutes for the SUROS discs and up to 4 hours for the railhead specimens, depending on the number of indentations taken for each sample. Large number of indents means a higher map resolution, which indicates a true representation of the material hardness as scarce data can highlight sporadic hard or soft spots which may be isolated hardness spots and not a representation of the surface hardness. Due to time limitation, each specimen was tested once and ideally multiple specimens from various sections of the railhead and SUROS cylinders should have been tested in order to introduce statistical variation into this study.

Figure 18 is a summary of the results from the hardness tests. The error bars indicate the minimum and maximum values measured for each specimen while the marker indicates the mean hardness value of each specimen. The R260 mean value is 273Hv which is the equivalent designated material hardness of around 260HB. For the R350HT material the mean value is the equivalent of 330HB, which is lower than the designated material hardness of 350HB, since it refers to the surface hardness, rather than the mean hardness. R350HT is a heat treated material, which varies in hardness from the centre of the railhead outwards, where the centre is the softest part of the railhead. This is captured in figure 16b where the centre of the railhead is softer (darker in colour), while figure 16a shows a more uniform distribution of hardness, with some isolated harder spots in the centre axis of the railhead. The results must be interpreted carefully when comparing the different materials as they all use the same colour range, however, the hardness range in figure 16a is 62Hv, while in figure 16b is 116Hv, almost double. This means that the isolated harder spots in R260 are not as significant as the hardness variation in R350HT. This is also evident by the error bars in figure 18, which show the range of hardness measured for R260 is smaller than the range of measurement in R350HT.

Materials A and C indicate a uniform distribution of sporadic harder areas, while material B exhibits a similar pattern to R350HT, which indicates a softer centre and this is confirmed by the hardness range of 120Hv, centre to edge of railhead. The hardness range for materials A and C is 94Hv and 72Hv respectively, indicated by the error bars in figure 18.

The SUROS specimens used for the hardness test have a diameter of 50mm. To produce the SUROS discs, the diameter is reduced to 47mm and the hardness near the circumference of the disc is of interest, since this is the contact face during the twin disc tests. The hardness difference between the industrial railhead and the laboratory SUROS disc can be seen in figure 18. In each case the hardness range on the SUROS is higher than the railhead, except for R350HT and material B. In all cases the mean hardness is slightly lower than the railhead mean hardness. The mean hardness might not be as important for this comparison, as explained the hardness near the circumference of the sample can influence the test as it is closer to the contacting face. The hardness maps in figures 16a-16e can provide a visual representation of the hardness distribution for the SUROS discs. The discs were made from the centre of railheads and this is evident in R260 where the isolated harder spots of the centre railhead are found in the SUROS disc. For R350HT and material B, part of the softer centre of the railhead is found concentrated in almost a third of the circumference of the SUROS discs, with about 100Hv hardness difference with the rest of the circumference. For materials A and C, although the hardness difference on the circumference can vary by around 100Hv, it is not concentrated but intermitted. The variable hardness on the running face, along with the intrinsic properties of material C, might have been the cause of the polygonal deformation and extreme wear that resulted from the twin disc testing at all slip conditions.
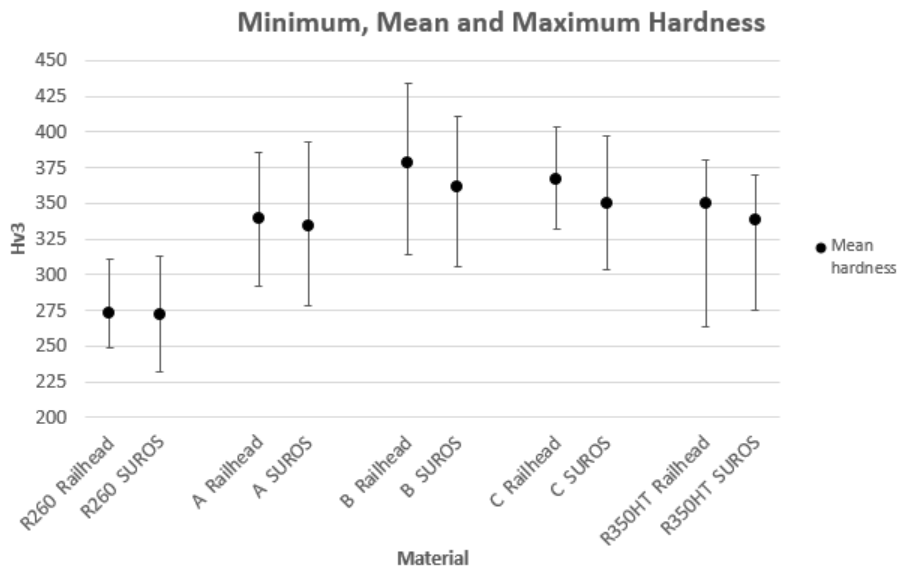
Figure 18 Hardness results for all materials

Further tests will be performed for accelerating the crack growth under rolling contact fatigue damage in order to evaluate the RCF performance of the premium material, as previously tested for R260 rail by Hardwick et al. [16]. Some rail materials are designed to have greater wear resistance and others to have greater RCF resistance, making it very difficult to optimise both. It has been discovered from premium rail trials in the field that the use of premium rail has unexpectedly changed the damage mechanism in particular locations from wear to RCF. This has identified a need for developing a new damage function describing the wear-RCF relationship with $T\gamma$ for the premium rails, going beyond the well-known damage function for standard rail [17].

6. CONCLUSIONS

Currently, wear coefficients have been utilised in mapping and predicting wear and RCF. This new data will be useful to make the required improvements to modelling tools based on wear coefficients and material properties [13]. This will eliminate the process of deriving wear coefficients from twin disc testing which is laborious and costly when it comes to exploring different scenarios with various loading conditions. Wear coefficients are limited to a single load, while mapping with dissipated energy $T\gamma$ the data can be extrapolated to various loading conditions. The purpose of this work is to provide a benchmark for comparison with other technologies such as laser cladding of alloys on wheels and rails, and to evaluate their performance. Previous work by Lewis et al. [12] on testing the wear of laser clad rail material has been very promising. In addition, this work will contribute to a database of information for wear prediction tools of premium material as well as laser clad material. Wear of wheel and rail discs for R260, four premium rails and a laser clad rail was measured in order to document its relationship to $T\gamma$ curves for three slip conditions of 1%, 10% and 20%. The wear resistance performance of these materials at high creepage and harsher conditions is of interest, as the premium materials are generally designed for high axle loads and tight curves. The wear rates produced in figure 6 correlate with the three wear regimes as identified by Lewis et al. [18] as mild, severe and catastrophic. At low slip tests, the premium materials are wearing at similar values and results can be inconclusive when the mass loss is low, without extensive and repeatable tests to produce a statistical analysis of multiple tests. At high slip tests of 10% and 20% the premium rails showed improved wear resistance over the standard rail, with material B to perform better, in line with the design intend of material B. Material C is designed for increased RCF resistance rather than wear and although at low slip the wear was moderately high, at high slip it exhibited high wear, outside of the other material's wear range.

Hardness mapping of railhead and SUROS specimens was conducted for direct comparison in their hardness distribution. Variation in hardness was identified in all SUROS specimens with R350HT and material B exhibiting distinct zones near the running face of lower/higher hardness, while all other materials exhibit sporadic low/high hardness on the running face. No direct conclusion can be drawn from the comparison of hardness distribution and wear from this data alone.

The wheel wear differs depending on the rail material and it is always higher than the rail wear due to the lower hardness of the wheel. Overall the ratio of wheel wear and rail wear varies with premium rail, showing more wheel wear with premium rail in comparison to standard rail, however the overall system wear may be reduced at low slip ratios but especially at high slip ratios, for example 20% (figure 7), which can be found in critical areas such as switches and crossings and tight curve track sections. R8 wheel material was used for all the tests. Different wheel material is in use by several train operators and future rail performance and comparison should include other wheel material, for comprehensive understanding of the in-service wear.

Further work on high slip would be of benefit to verify the performance of this early study, with focus on both the rail and wheel wear performance and preferably in full scale testing to eliminate the limitation of small scale testing. In a study where a large number of samples can be tested, separating the results into initiation phase (newly installed, work hardening phase) and steady state would make it clearer how each material performs. The RCF performance of the rail has not been evaluated in this study and it is important that future work investigates the RCF performance in combination with the wear performance. In addition, work hardening effects of the different rails need to be considered when selecting premium rails.

The combination of the above data can be of benefit to the industry when selecting rail material for various sections of railway.

7. REFERENCES

[1]   M. F. Ashby and S. C. Lim, "Wear- mechanism maps," *Scripta Metallurgica et Materiala,* vol. 24, no. 5, pp. 805-810, 1990.

[2]   R. Lewis and U. Olofsson, "Mapping rail wear regimes and transitions," *Wear,* vol. 257, no. 7-8, pp. 721-729, 2004.

[3]   J. F. Archard, "Contact and Rubbing of Flat Surfaces," *Journal of Applied Physics,* vol. 24, no. 8, pp. 981-988, 1953.

[4]   R. Lewis *et al.*, "Towards a Standard Approach for Wear Testing of Wheel and Rail Materials," *Proceedings of the Institution of Mechanical Engineers, Part F: Journal of Rail and Rapid Transit,* vol. 231, no. 7, pp. 760-774, 2017.

[5]   M.Burstow, "Whole Life Rail Model Application and Development for RSSB: Development of an RCF Damage Parameter," Rail Safety & Standards Board, Derby, AEATR-ES-2003-832, 2003, issue 1.

[6]   M. Steenbergen, M. Hiensch, and M. Steenbergen, "Rolling Contact Fatigue on premium rail grades: Damage function development from field data," *Wear,* vol. 394, pp. 187-194, 2018.

[7]   R. Pippan and R. Stock, "Rail grade dependent damage behaviour – Characteristics and damage formation hypothesis," *Wear,* vol. 314, no. 1-2, pp. 44-50, 2014.

[8]   R. Pippan and R. Stock, "RCF and wear in theory and practice—The influence of rail grade on wear and RCF," *Wear,* vol. 271, no. 1-2, pp. 125-133, 2011.

[9]   T. M. Beagley, "Severe wear of rolling-sliding contacts," (in English), *Wear,* Article vol. 36, no. 3, pp. 317-335, 1976.

[10]   H.-K. Jun, S.-J. Kwon, D.-H. Lee, and J.-W. Seo, "Rolling contact fatigue and wear of two different rail steels under rolling–sliding contact," *International journal of fatigue,* vol. 83, pp. 184-194, 2016.

[11]   P. J. Bolton and P. Clayton, "Rolling sliding wear damage in rail and tyre steels," (in English), *Wear,* Article vol. 93, no. 2, pp. 145-165, 1984.

[12]   S. R. Lewis *et al.*, "Improving rail wear and RCF performance using laser cladding," (in English), *Wear,* Article; Proceedings Paper vol. 366, pp. 268-278, Nov 2016.

[13]   R. Lewis *et al.*, "Mapping railway wheel material wear mechanisms and transitions," *Proceedings of the Institution of Mechanical Engineers, Part F: Journal of Rail and Rapid Transit,* vol. 224, no. 3, pp. 125-137, 2010.

[14]   W. J. Brayshaw, M. J. Roy, T. Sun, V. Akrivos, and A. H. Sherry, "Iterative mesh-based hardness mapping," (in English), *Science and Technology of Welding and Joining,* Article vol. 22, no. 5, pp. 404-411, 2017.

[15]   P. J. Blau, "How common is the steady- state? The implications of wear transitions for materials selection and design," *Wear,* vol. 332-333, pp. 1120-1128, 2015.

[16]   C. Hardwick, R. Lewis, and D. T. Eadie, "Wheel and rail wear—Understanding the effects of water and grease," *Wear,* vol. 314, no. 1-2, pp. 198-204, 2014.

[17]   M. Burstow, "Experience of premium grade rail steels to resist rolling contact fatigue (RCF) on GB network," *Ironmaking & steelmaking,* vol. 40, no. 2, pp. 103-107, 2013.

[18]   R. Lewis and R. S. Dwyer-Joyce, "Wear mechanisms and transitions in railway wheel steels," (in English), *Proceedings of the Institution of Mechanical Engineers Part J-Journal of Engineering Tribology,* Article vol. 218, no. J6, pp. 467-478, Dec 2004.